ISSN 2176-5480

22nd International Congress of Mechanical Engineering (COBEM 2013)
November 3-7, 2013, Ribeirão Preto, SP, Brazil

COMPUTATIONAL ANALYSES OF SANDWICH STRUCTURES UNDER 3-POINT BENDING TESTS

Mauricio Francisco Caliri Junior
Felipe Godoy de Carvalho
Volnei Tita
Aeronautical Engineering Department - Sao Carlos School of Engineering – University of São Paulo – Av. João Dagnone, 1100 , São Carlos - SP - Brasil
mjcaliri@sc.usp.br; voltita@sc.usp.br

Marcelo Leite Ribeiro
Aerospace Engineering - Federal University of Santa Catarina - Rua Prudente de Moraes 406, Joinville, Brasil.

Abstract. *This paper discusses the modeling of sandwich structures with core made from rigid anisotropic polymeric foam under 3-point bending tests. It also contains a discussion about material models and the entire calibration procedure of the parameters involved. First, specimens of poly (vinyl chloride) (PVC) foam are investigated through experimental analyses in order to understand the anisotropic mechanical behavior of the cellular structure. Then, isotropic material models available in the finite element software Abaqus™ are evaluated in order to verify their potentialities and limitations in modeling anisotropic foams and how the related parameters can influence the results. Due to material anisotropy, it is possible to obtain different values for the same parameter in the identification process. Thus, it is necessary to calibrate the parameters of the material model according to the application of the structure. The models investigated showed minor and major limitations to simulate the mechanical behavior of the sandwich structures under bending and shearing loads. Results showed that the calibration process and the choice of the material model applied to simulate the rigid polymeric foam can provide good quantitative results and save time during the project development of sandwich structures.*

Keywords: *Finite Element Analyses; Material model; Foams; Crushing; Plastic behavior*

1. INTRODUCTION

The numerical modeling of sandwich structures is based on the study of their components: the skins, the core and the interfaces. It is not a trivial task to design a sandwich structure with skins manufactured in laminate composite material and a polymeric light core (foam).

Researchers have usually approached the scope of sandwich structures by choosing one of its main components to focus on and they use one of the methods: numerical, analytical and/or experimental (Russo and Zuccarello, 2007; Sadighi *et al*., 2007; Shipsha *et al*., 2003; Soden, 1996 Sokolinsky *et al*., 2004; Swanson and Kim, 2002; Tagarielli *et al*., 2004; Yang *et al*., 2001; Zenkert *et al*., 2004).

This paper contributes to the scope of sandwich structures with the calibration of phenomenological models for the core, which is made of polymeric foam. Thus, 3-point bending experimental results of a particular sandwich structure were used to validate the numerical results obtained through Finite Element Analyses (FEA). These FEA models were built with a new and unique strategy to identify and calibrate the material model parameters for the particular foam. More specifically, the structure under investigation is composed of laminate skins (composite material made with epoxy resin reinforced by glass fibers) and a polymeric core. Such core is a rigid poly (vinyl chloride) (PVC) foam (Divinycell H60). The anisotropic microscopic features of this foam were investigated in previous works developed by the present authors (Caliri Junior *et al*., 2012; Caliri Junior *et al*., 2010; Tita and Caliri Jr., 2013; Tita and Caliri Junior, 2012; Tita *et al*., 2012). These features impact on the macroscopic response of this cellular material, which exhibited anisotropic mechanical behavior. Moreover, numerical and computational issues were investigated, because large strains under the indenter area appeared in the core during 3-point bending tests. Hence a review on finite element topics such as shear locking in bending and implementation of hardening laws and flow rules is advised. Despite of the calibration procedure of the parameters involved in the simulations, the numerical results matched the experimental ones with good accuracy. As a topic for future works, the influence of the adhesive layer in the sandwich structure response was also approached numerically.

2. MATERIALS

The core of the sandwich structure is rigid PVC foam manufactured by DIAB (DIAB, 2010) and named as Divinycell H60. The skins comprised three bidirectional composite layers (woven fabric) made of glass fiber and epoxy matrix (Fig. 1).

ISSN 2176-5480

In the experimental 3-point bending tests, a 100 mm span was firstly adopted. Then, 150 mm span tests were carried out too. In Table 1, it is possible to observe that the sandwich structure under study has typical dimensions. The thickness "*t*" of the skins is much smaller than the core's "*c*", which is much smaller than the sandwich's length "*L*" ($t<<c<<L$). Based on these geometrical relations, the main failure mode of this structure should be indentation of the core during 3-point bending tests (Steeves and Fleck, 2004a, b; Mendonça, 2005). These experimental tests were carried out using displacement control and the force was applied very slowly (1 mm/min), performing quasi-static tests.

Table 1. Average nominal dimensions of the sandwich components

Material	Core	Skin
	Divinycell H60	3 bidirectional plies (glass fiber/epoxy resin)
Length (mm)	250	250
Width (mm)	30	30
Thickness (mm)	10	0.22

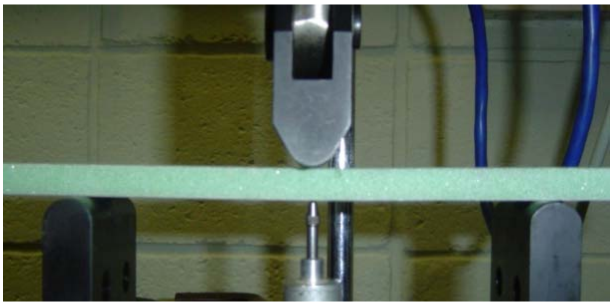

Figure 1. 3-point bending setup

2.1 Polymeric core

It must be pointed out that this particular polymeric core has a transversely isotropic mechanical behavior (Caliri Junior *et al*., 2012; Caliri Junior *et al*., 2010; Tita and Caliri Jr., 2013; Tita *et al*., 2012). Moreover since this foam is a lightweight core (low density, 60 kg/m³) the influence of its anisotropy cannot be neglected. The difference in strength and stiffness, considering the direction of the loading, can be twice as high. Foams and cellular materials, manufactured through foaming agents (CO_2, HFCCs, Pentens or HFCs, for instance), have microstructures, which are vulnerable to gravity during the manufacturing process (Química e Tecnologia dos Poliuretanos, 2010; Gibson and Ashby, 1988; Weaire and Hutzler, 1999).

In Fig. 2, there is a sample of the core's foam investigated and the material indexes. The out-of-plane direction is indexed by number 3. Also, it is possible to observe the microstructures of in-plane section (directions 1-2) and out-of-plane section (directions 1(2)-3). These images can help explaining the difference in stiffness and strength of this PVC foam, considering the loading direction.

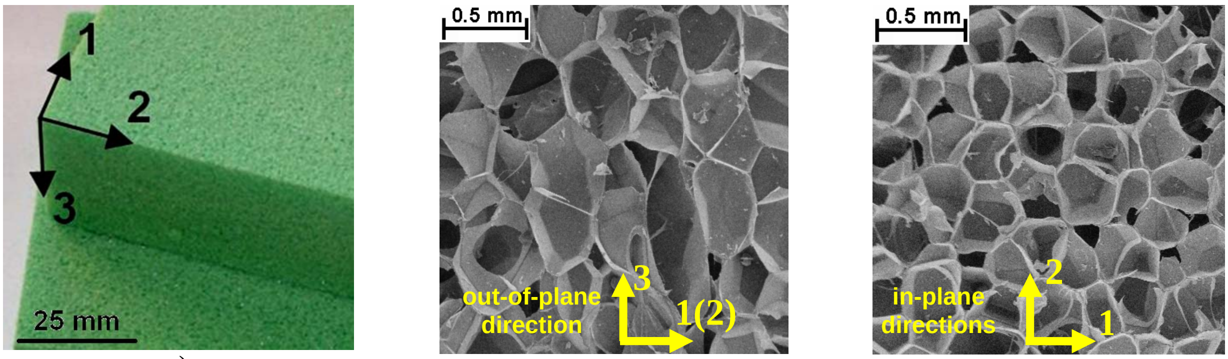

a) b) c)

Figure 2. Divinycell H60 foam: (a) plates from DIAB; transversely isotropic micrographs of the PVC foam showing the microstructure pattern of the cells in each plane: (b) out-of-plane section (plane 3-1); (b) in-plane section (plane 1-2)

ISSN 2176-5480

Therefore, as expected, the response of this foam differs according to the loading path. Under tension, the material shows a brittle behavior and under compression, it can be considered as perfect plastic up to the beginning of densification of the cellular structure due to the crushing of the cells. Figures 3(a) and 3(b) depict the uniaxial mechanical behavior of Divinycell H60 investigated in Tita et al. (2012).

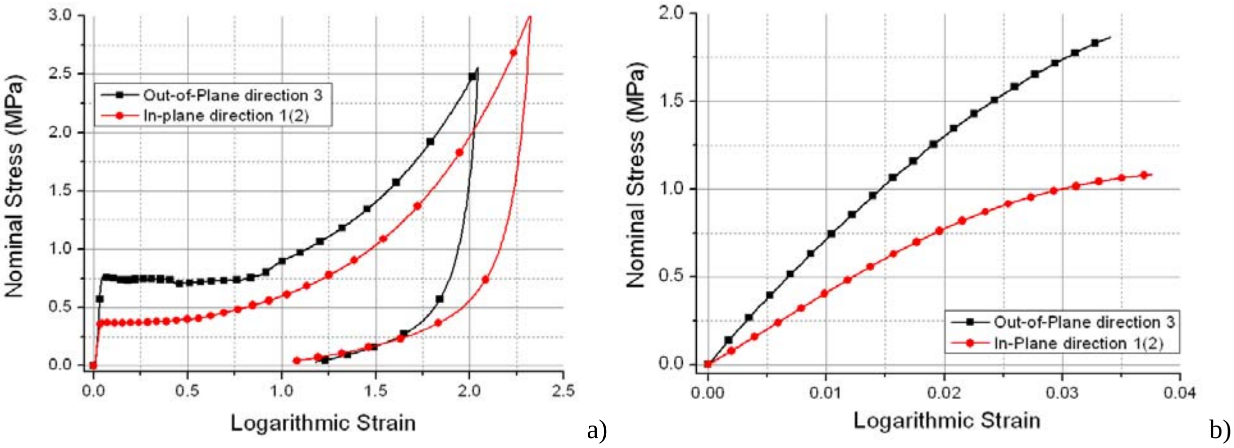

Figure 1. Divinycell H60 Mechanical behavior: (a) Compression; (b) Tension

2.2 Skins and adhesive

The skins comprise a staking of three plies and each ply is a glass fiber reinforced composite with an epoxy matrix. In fact, bidirectional woven fabrics were used in the common hand-lay-up manufacturing process in order to obtain the composite skins with the stacking sequence: $[0º/45º/0º]_T$ (Oliveira, 2007). Hence, the relations $E_{11} = E_{22}$ and $\nu_{13} = \nu_{23}$ can be applied (Mendonça, 2005). Following the procedures established by ASTM D3029 and D3518, Oliveira (2007) obtained the Young's modulus (E_{11}) and the shear modulus (G_{12}) as well as the strength values under tension (X_{T1}) for this composite material (Tab. 2).

Table 2. Mechanical properties of the fiber glass/epoxy composite ply

ASTM D3039/D3518	E_{11} (GPa)	υ_{12}	G_{12} (GPa)	$X_{T1} = X_{T2}$ (MPa)
Average values	26.5	0.16	4.25	419

Based on the nominal thickness of the laminate, 0.22 mm (Oliveira, 2007), each ply thickness may be considered equal to 0.0733 mm. This value was used in the computational models for each ply thickness. Even though the strength of each ply is given in Tab. 2, these values are listed for post processing analyses only, because the laminates (skins) were later modeled in the FEA analyses as a linear elastic material without any failure assumptions.

Regarding the adhesive between core and skins, this component was initially not simulated. However, as a cellular structure, the core has only 4-5% of solid material within the respective foam volume. It is possible that some of this void area was filled with adhesive during the assemblage process, even though the foam is a closed-cell (Gibson and Ashby, 1988) type of cellular structure. Inside the foam, the adhesive stiffens the region next to the skins, changing the effective stiffness and also possibly the strength of the sandwich structure.

Studying Fig. 2, the adhesive's average thickness should be less than 0.5 mm. Nonetheless, this value should be confirmed with statistical analyses of SEM (Scanning Electron Microscopy) images of this sandwich structure.

3. MATERIAL MODELS

Computational modeling of sandwich structures with lightweight cores (foams) requires a broader understanding of material models. These cores can be modeled macroscopically as continuous solid materials instead of modeling the microstructures of the cellular material (Abrate, 2008; Gibson *et al.*, 1989; Gioux *et al.*, 2000; Miller, 2000; Triantafillou *et al.*, 1989; Wang and Pan, 2006; Zhang, *et al.*,1998). This is a regular practice because detailing the micro structure and then allowing the FEA analysis to estimate the macroscopic response of the cellular structure is a huge challenge (Gong *et al.*, 2005; Gong and Kyriakides, 2005). Also, the computational time would increase substantially and the effectiveness of the solutions could be jeopardized due to the approach taken. Therefore, in this work, the cellular material is modeled as a continuous solid material. However, the material model has to be chosen considering all the phenomenological responses of the PVC foam. Different behaviors under compression and tension

ISSN 2176-5480

loadings, created due to the anisotropy (transversely isotropic), restrict the choices of material models. These material models have parameters, which must be carefully calibrated to obtain reliable results, especially for large logarithmic strains ($\varepsilon > 100\%$).

Abaqus™ is chosen to perform the numerical analyses, because this commercial FEA code contains material models implemented for crushable foams based on the works of Deshpande and Fleck (Deshpande and Fleck, 2000, 2001). There is an authentic representation of Deshpande and Fleck's model in Abaqus™, which is named *Crushable Foam with Isotropic Hardening (CIH)*. However, there is also an implemented version of this model, which is slightly modified to account for the brittle response under tension and the high strain energy capacity of foams under compression, which is named *Crushable Foam with Volumetric Hardening (CVH)*. On the one hand, the changes in this latter model create limitations in the modeling of multi-axial and local loads for large strains. On the other hand, these changes allow for a better description of anisotropic behaviors such as that of the polymeric foam herein studied. The material model implemented is represented by the yield surface written in Eqs. (1) and (2) and plotted in Fig. 4.

$$f = [\sigma_v^2 + \alpha^2(\sigma_m - \sigma_0)^2] - [1 + (\alpha/3)^2]\sigma_y^2 \leq 0 \tag{1}$$

$$\sigma_v = \left(3S_{ij}S_{ij}/2\right)^{1/2};\ \sigma_m = -(\sigma_{kk}/3) \tag{2}$$

In Eqs. (1) and (2), σ_v is known as the von Mises equivalent stress; σ_m is the mean stress; σ_0, α and σ_y are adjusted by experimental analyses. S_{ij} is the second invariant of stress deviator tensor. More details can be found in the Abaqus /CAE User's Manual (2007).

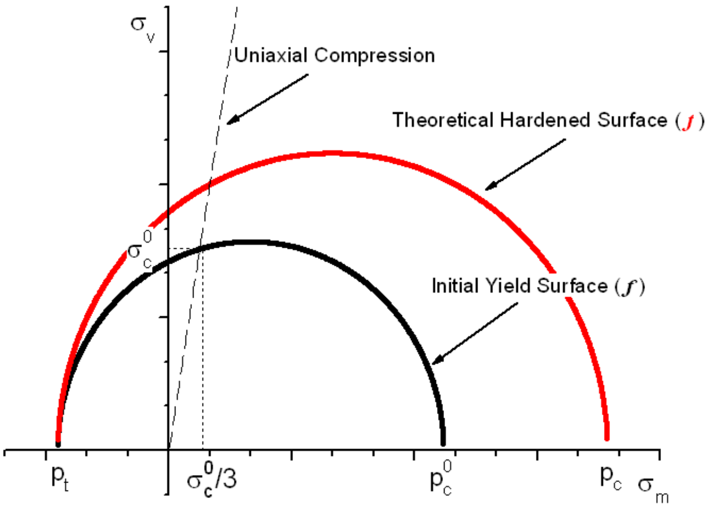

Figure 4. Volumetric model: Initial yield surface and theoretical hardened surface

Figure 4 depicts the initial yield surface and a new theoretical hypothetical yield surface, representing the hardened material. P_t refers to the negative hydrostatic tension yield stress and P_c is the positive hydrostatic compressive yield stress. The term theoretical was used because the hardening in the Fig. 4 does not represent what is implemented in the software Abaqus™. In fact, for null or negative mean stress contributions (tension hydrostatic stress), the surface does not yield and the material is assumed to be perfect plastic (Abaqus /CAE User's Manual, 2007). However, when the mean stress contributions are positive, i.e., for compressive loadings, the surface evolves at the right side of the stress plane according to the Volumetric Hardening.

Such approach is based on the fact foams usually have a hydrostatic compressive yield stress much larger than the correspondent hydrostatic tension yield stress (Abaqus /CAE User's Manual, 2007). The implementation in Abaqus™ suggests that this limit in tension is about 5 to 10% of the compression one. In these cases, the gap between the yield surfaces is negligible up to some extent (Caliri Junior, 2010). Besides, adding the fact that crushable materials usually behave in a perfect plastic manner up to large logarithmic strains (higher than 100%), the original yield surface does not evolve so much and the gap is nearly zero. These assumptions must be carefully followed mainly for tension and shearing loads. If the cellular material presents a strong hardening and/or, if the hydrostatic tension yield stress is higher than the 5-10% of the compressive yield stress, then, under multi-axial loadings, the material model algorithm is likely to crash. The reason lies on the fact that the discussed gap in the material model will be too large to be neglected. Managing element type, size, order, and mesh density can control the model convergence to circumvent or overcome such gap debility in the material model implementation.

ISSN 2176-5480

Reviewing the discussed yield surface (Eq.1), the parameters can be determined with experimental analyses. The material's yield stress (σ_y) is evaluated by using uniaxial tests. σ_0 is the translation value of the yield stress in the mean stress axis, value on the abscissa coordinate (a type of Kinematic Hardening) (Chen and Han, 1988). The parameter α is the most intricate one. Equations (3) to (5) define this parameter and its relation to the shape of the yield surface (Abaqus /CAE User's Manual, 2007).

$$\alpha = 3k/\sqrt{(3k_t + k)(3 - k)} \tag{3}$$

$$k = \sigma_c^0/p_c^0 \tag{4}$$

$$k_t = p_t/p_c^0 \tag{5}$$

The parameters k and k_t are the actual parameters to be adjusted experimentally within Abaqus^{TM} along with the hardening curve. As for the elastic phase, the material is considered isotropic and the elastic Poisson's ratio and Young's modulus are required as usual. In the plastic regime, the CVH model assumes a null plastic Poisson's ratio, which locks the control over the flow potential. A control over the shape of the yield surfaces through the ratio k and k_t is offered instead. An initial isotropic yield surface can be defined in the CVH model by setting σ_0 equal to "0" and k_t equal to "1".

Definitions of k and k_t parameters must be well understood. The first one is the quotient of the initial yield stress in uniaxial compression (σ_c^0), and the initial yield stress in hydrostatic compression (p_c^0) as shown by Eq. (4). The second one is the quotient of the yield stress in hydrostatic tension (p_t), and the initial yield stress in hydrostatic compression (p_c^0) as shown by Eq. (5). The hydrostatic tension does not carry the super script "0", because the yield surface does not evolve under null or tensile mean stresses. Based on k and k_t values, Abaqus^{TM} can estimate the current yield surface for each material point in the FE model of the foam.

A short investigation of this material model's parameters was conducted by Oliveira *et al.* (2008) with uniaxial compressions. Rizov (2006a, b) also worked with this material model in Abaqus^{TM}, but the author did not detail the input data parameters. It is believed that Rizov used the isotropic hardening model in his simulations. Also, in the previous works of the present authors, it is possible to find more details about these material models (Tita and Caliri Junior, 2012).

To complete the input data set for the CVH material model, a table containing the logarithmic plastic strain and the correspondent Cauchy stress must be provided in Abaqus^{TM} in order to control the evolution of the yield surface of both material models. The values required by the table in Abaqus^{TM} can be completed by using the data of uniaxial compression tests.

4. THREE-POINT BEDING TESTS AND FINITE ELEMENT SIMULATIONS

Extending the previous work of Tita and Caliri (2012) to sandwich structures and based on the results of Tita *et al.* (2012), two sets of parameters were identified to calibrate the CVH material model and then simulate the core of the sandwich structure under 3-point bending simulations. Based on these parameters, two yield surfaces were created to represent the anisotropic non-elastic behavior of the PVC foam using the CVH material model. To determine these yield surfaces, three experimental values were required and obtained from Tita and Caliri (2012). These values can be seen in Tab. 1. UCYS corresponds to the uniaxial compression yield stress, UTYS corresponds to the uniaxial tension yield stress and HCYS corresponds to the hydrostatic compression yield stress. In addition, it is possible to observe the values for the k and k_t parameters and the linear elastic regime Poisson's ratio (υ_{el}) and Young's modulus (E).

Table 3 - Parameters for the 3-point bending tests using the CVH material model

Surface set	UCYS (MPa)	UTYS (MPa)	HCYS (MPa)	E (MPa)	υ_{el}	k	k_t
I	0.75	1.96	0.45	53	0.30	1.8852	12.2965
II	0.57	1.52	0.45	38	0.21	1.9418	5.6858

The first yield surface (I) was defined with the "out-of-plane set of properties", i.e., the load was applied in the out-of-plane direction (3) in the experimental tests. Then, in an attempt to improve the results of numerical simulations considering the multi-axial loads created by the indenter, a second yield surface (II) was defined. For this second surface, the results from in-plane and out-of-plane experimental tests of the foam were properly averaged. (Tita and Caliri, 2012).

Figure 5 shows the FE model of the 3-point bending for the sandwich structure. One can also see the boundary conditions applied to the rigid supports, indenter and the flexible sandwich structure. The supports were clamped and

ISSN 2176-5480

the indenter is free to move only vertically. A contact model was used to simulate the interactions between the rigid supports and indenter part and the flexible sandwich structure. These interactions were defined as smooth tangential contact (frictionless). After inspection of the surfaces involved in the experimental setup, it was observed that this latter assumption was reasonable.

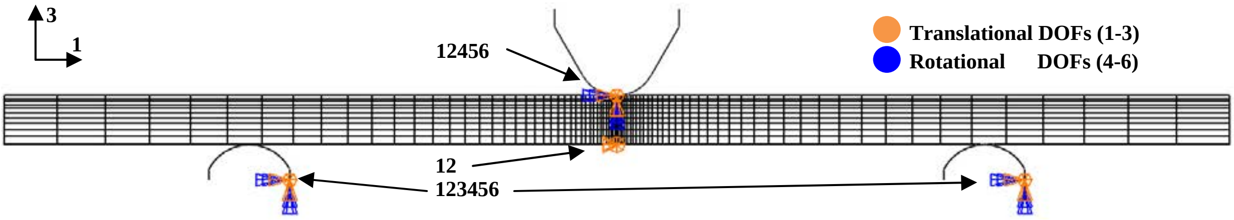

Figure 5. Finite element model of the sandwich structure: mesh and constrained degrees of freedom (DOFs)

Using the nominal data from Fig. 3, Tab. 2 and Tab. 3, four FE models were developed to assess the numerical performance of the CVH model applied to sandwich structures. Each FE model is defined according to span length (100 mm or 150 mm) and the yield surface (I or II) used to simulate the core.

To evaluate the performance of the numerical simulations, the experimental Force per Displacement curves for both span lengths are plotted in Fig. 6. The vertical displacements were measured by a LVDT beneath the lower skin.

At first, the adhesive layers are neglected and the nominal sandwich was modeled for both spans and surface sets. Then, based on the fact that the out-of-plane core's elasticity modulus is 53 MPa, the authors decided to consider modeling the adhesive layers. What motivated this approach is the fact that common values for Young's modulus of polymeric adhesives are in between the range of 1 to 5 GPa (Mendonça, 2005; Ribeiro, 2009). This value is nearly 20 times the highest modulus of the core.

To model the adhesive, a fourth layer in the skins, inserted next to the core, was modeled as an isotropic material with elasticity modulus of 1485 MPa and Poisson ratio of 0.35 (Ribeiro, 2009). The average thickness is assumed to be half the maximum expected thickness, hence 0.25 mm. To maintain the overall thickness of the sandwich, the core thickness was reduced to 9.5 mm in these simulations.

Although these values need confirmation, they can indicate whether or not the adhesive does in fact contribute to the sandwich's stiffness and strength. The authors decided to evaluate the strength of the sandwich structures indirectly, i.e., their strengths were defined as the highest reaction force in the 3-point bending tests, despite possible failure initiation before this peak load.

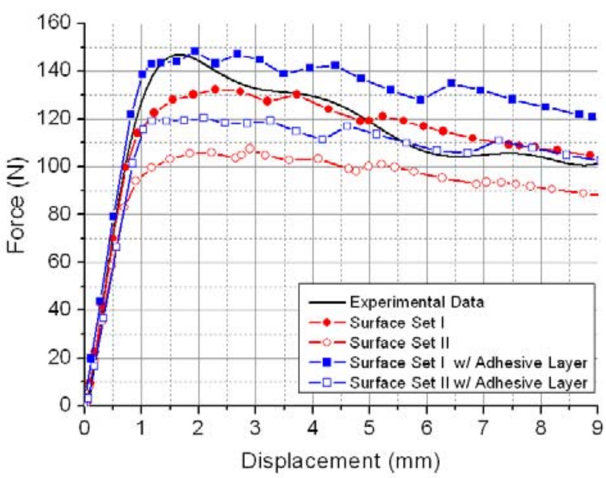

a)

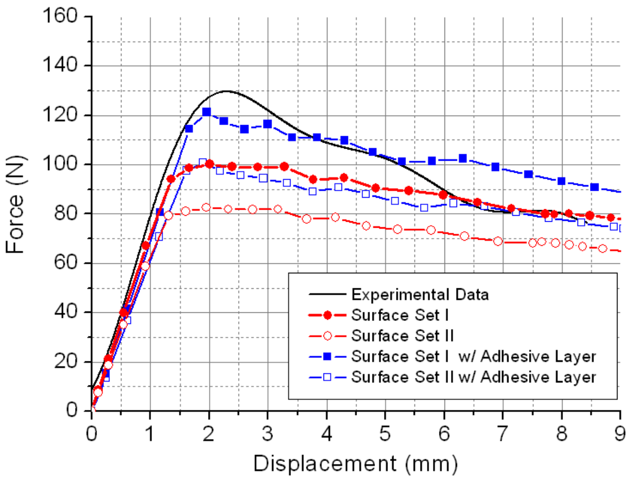

b)

Figure 6. Comparison between experimental and numerical results for: a) 100 mm span test; b) 150 mm span test

In both graphs in Fig. 6, one can see that the elastic regime is better represented numerically in the 100 mm span models. The simulations of the 150 mm span test predicted a load peak lower than the real response of the structure.

Specifically in Fig. 6a, the surface set I provided better results. This is expected because the linear elastic response deals with small strains and the load on the structure is mainly applied in the normal direction, i.e., in direction 3 of the foam. Hence, a stiffer response is expected.

ISSN 2176-5480

The addition of the estimate adhesive layer improved the results considerably. With these findings, it is recommended that further studies on sandwich structures with low weight cores should properly incorporate the adhesive's contribution to the core's stiffness and strength.

Regarding the Fig. 6b, the same pattern of Fig. 6a is seen. Nonetheless the numerical results did not show the same precision for the 150 mm span models. These curves also endorse the need for representation of the bonding layer. In attempt to measure the actual thickness of the skins, a sample from one of the tested sandwich specimens was removed and hand polished. Three measures of this sample provided an average value of 0.33 mm. However, despite the efforts of the authors to measure only the thickness of the skin, it is not wise to assert that this measure contains only material from the skin. It is believed that a portion of this new skin thickness is due to the adhesive used to glue the skins to the core. Thus, the authors are unsure about the actual thickness of the skins and the adhesive. Only with statistical micro analysis of the sandwich structure one can provide the answer. This micro analysis will be carried out in future works.

An insight into the results suggests that the sandwich structure is likely to fail through failure of the upper skin. Since the skins were modeled as linear elastic materials, the curves in Fig. 6 are valid up to a maximum of 1 and 2 mm displacement of the lower skin, respectively.

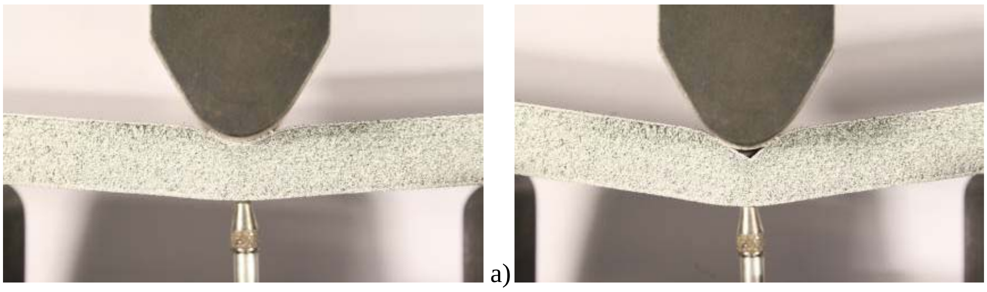

a) b)

Figure 7. 3-point bending test of the sandwich structure with 100 mm span.; a) at ~4mm displacement; b) Total failure of the upper skin at ~8mm

In Fig. 7, two photos of the actual 3-point bending test are seen for approximately 4 and 8 mm displacement of the lower skin. It was verified that the sandwich structures gradually lose stiffness and strength during tests up to maximum reaction force of 145 N (for the 100 mm span case). Past this peak load, the overall failure of the sandwich structure is intensified until total failure occurs. This is indicated by the rupture of the upper skin and the appearance of a "V" pattern (Fig. 7b) formed by the loose edges.

Figure 8 shows the longitudinal (direction 1) principal stress results (100 mm span) for nominal and adhesive settings. In the first case, the stress is high enough to damage the top ply of the upper skin since its strength is 419 MPa according to Tab. 2. For the second case, the stress is lower but still strong enough to locally damage the epoxy matrix (typical compression strength values range from 100 to 200 MPa and tensile strength values range from 50 to 100 MPa, see Mendonça (2005)). This endorses the conclusion that the polymeric matrix is already damaged before the peak load is achieved in both bending tests.

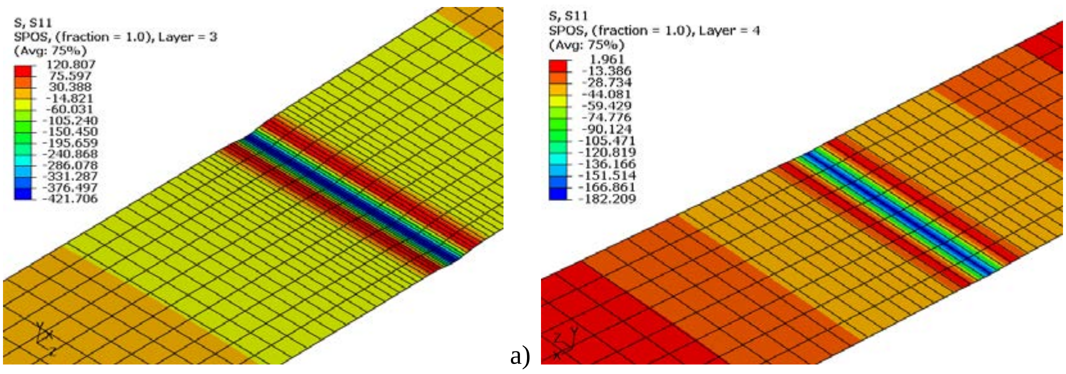

a) b

Figure 8. Longitudinal stress S_{11} (stress in direction 1): a) Third ply of the top skin - nominal settings at 1.00 mm displacement; b) Fourth ply of the top skin - adhesive settings at 0.92 mm displacement

Inspection of the adhesive layers indicates a longitudinal nominal stress much lower than those shown in Fig. 8. That is because the adhesive layer is closer to the core and the influence of the external load is weakened throughout the plies until the adhesive interface is reached.

ISSN 2176-5480

To support the numerical results provided by the FE model with the adhesive layer, the plastic strain in the direction 2 in plotted in Figs. 9-10. Two displacement levels were chosen to be evaluated. These levels are as close as possible to those shown by Fig. 7 to allow a direct comparison.

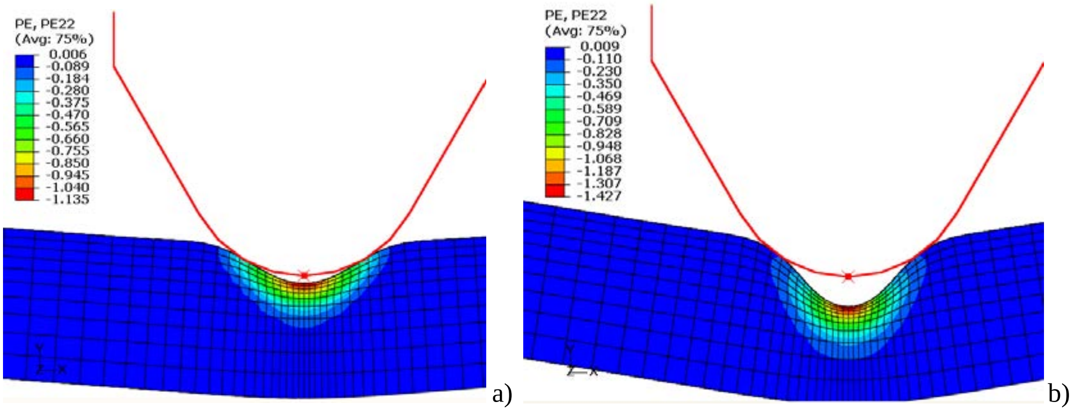

Figure 9. Plastic strain in the core for 3-point bending simulation of the sandwich structure with nominal settings and 100 mm span; a) at 3.8 mm displacement; b) at 8.0 mm displacement

It can be verified that for the FE models with adhesive layers within the skins, the indenter keeps a larger area of contact with the upper skin during the numerical simulations of the 3-point bending test (Fig. 10). This is in better agreement with experimental results than the results for the simulation using the nominal thickness of the skins (Fig. 9).

Based on Figs. 6 to 10, it is likely that the mechanical contribution of adhesive used to bond the skins to the core cannot be neglected for this sandwich structure. These results strongly point the need for a better mechanical investigation of the epoxy matrix within the composite skin and the adhesive as well.

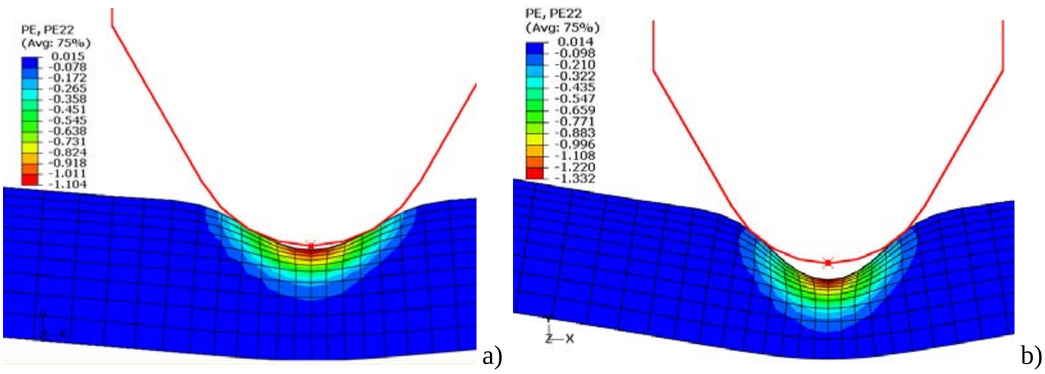

Figure 10. Plastic strain in the core for 3-point bending simulation of the sandwich structure with corrected settings and 100 mm span; a) at 4.1 mm displacement; b) at 8.0 mm displacement

5. CONCLUSION

Modeling sandwich structures is a very delicate task especially in the case of concentrated loads and failure analysis of sandwich structures with lightweight cores (foams). Overlooking the implementation assumptions of phenomenological material models may hinder the use of such models due to the amount of numerical issues that may arise. Even if a solution is achieved, the results might be questionable or even useless depending on the data needed in the post processing analyses.

For the sandwich structures simulated in this work, the best results were seen for the 100 mm span model with surface set I and with the adhesive layer included. Although the surface set II did not provide good results for these sandwich beams in 3-point bending tests, analyses of other sandwich structures submitted to a different multi-axial loading might point otherwise.

It was also shown that these sandwich structure constructions with very light polymeric cores are sensitive to the thickness and mechanical properties of the adhesive layer. This conclusion is based on the fact the adhesive layer is usually stiffer and stronger than cores made of polymeric foam.

A note should be made regarding the dimensions of the sandwich structures tested. Perhaps the last statement may not be true if the sandwich dimensions were similar to those of a square plate, not a rectangular beam. Then, the mechanical contribution of the adhesive could indeed have been neglected.

Therefore, the authors highly recommend a careful investigation of elastic-plastic-failure parameters and propose a calibration step for numerical simulation of lightweight composite sandwich structures with polymeric core.

6. ACKNOWLEGMENTS

The authors would like to thank CNPq (133595/2008-0) and FAPESP (2009/00544-5) for the financial support, and also, Professor Reginaldo Teixeira Coelho for providing a license of software Abaqus™.

7. REFERENCES

Abaqus /CAE User's Manual, 2007. *ABAQUS version 6.7 - documentation.* © Dassault Systèmes.

Abrate, S, 2008. Criteria for yielding or failure of cellular materials. *Journal of Sandwich Structures and Materials*, v. 10, p. 5.

Caliri Junior, M. F. 2010. *Modelos de material para espumas poliméricas aplicadas a estruturas aeronáuticas em material compósito sanduíche*. Dissertação (Mestrado em Engenharia Mecânica) - Universidade de São Paulo, Conselho Nacional de Desenvolvimento Científico e Tecnológico. Orientador: Volnei Tita.

Caliri Júnior, M. F.; Soares, G. P.; Angélico, R. A.; Canto, R. B.; Tita, V., 2012. Study of an anisotropic polymeric cellular material under compression loading. *Materials Research*, v. 15, p. 359-364.

Caliri Junior, M.F. ; Tita, V. ; Angelico, R. A. ; Canto, R. B. ; Soares, G. P., 2010. Study of an anisotropic polymeric cellular material under compression loading. *In:* Congresso Brasileiro de Engenharia e Ciência dos Materiais, 2010, Campos do Jordão. Anais do XIX CBECiMAT.

Chen, W.F.; Han, D.J., 1988. *Plasticity for structural engineers.* New York: Springer-Verlag.

Deshpande, V.S.; Fleck, N.A., 2001. Multi-axial yield behaviour of polymer foams. *Acta materialia*, v. 49, p.1859.

Deshpande, V.S.; Fleck, N.A.,2000. Isotropic constitutive models for metallic foams. *Journal of the Mechanics and Physics of Solids*, v. 48, p. 1253.

DIAB, 2010. Literature - Manuals. Technical Manual: Divinycell H. Mar. 2nd, 2010. <http://www.diabgroup.com/europe/literature/e_lit_man.html>.

Gibson, L. J.; Ashby, M. F.; Zhang, T. J.; Triantafillou, T. C., 1989. Failure surfaces for cellular materials under multiaxial loads -I. Modelling. *International Journal of Mechanical Sciences*, v. 31, n. 9, p. 635.

Gibson, L. J.; Ashby, M., 1988. *Cellular solids*: structures & properties. England: Pergamon Press-Headington Hill Hall.

Gioux, G.; Mccormack, T.M.; Gibson, L.J., 2000. Failure of aluminum foams under multiaxial loads. *International Journal of Mechanical Sciences*, v. 42, p.1097.

Gong, L.; Kyriakides, S., 2005. Compressive response of open cell foams Part II: Initiation and evolution of crushing. *International Journal of Solids and Structures*, v. 42, p. 1381.

Gong, L.; Kyriakides, S.; Jang, W. -Y., 2005. Compressive response of open-cell foams. Part I: Morphology and elastic properties. *International Journal of Solids and Structures*, v. 42, p. 1355.

Matweb, 2013. Material property data. Mar 16th 2013. <www.matweb.com>.

Mendonça, P. T. R., 2005. *Materiais compostos e estruturas sanduíche:* projeto e análise. Barueri: Manole.

Miller, R. E. A., 2 00. continuum plasticity model for the constitutive and indentation behaviour of foamed metals. *International Journal of Mechanical Sciences*, v. 42, p.729.

Oliveira, G. P. et al., 2008. "An investigation of material model parameters for foams of composite sandwich structures". *In:* CONGRESSO NACIONAL DE ENGENHARIA MECÂNICA. 5., 2008. Salvador. *Anais*… Salvador: ABCM, 2008.

Oliveira, G. P., 2007. *Evaluation de modèles de matériaux des structures sandwiches aéronautiques.* São Carlos: EESC/France: Dép. Génie Mécanique - Université Pierre et Marie Curie, 49 p. (Internacional internship report).

Química e Tecnologia dos Poliuretanos., 2010. May 20th 2010. <http://www.poliuretanos.net/>.

Ribeiro, M. L., 2009. Software for analyses of bonded joints: composite-composite and metal-composite. 163p. *Thesis (Master)* - School of Engineering of São Carlos, University of São Paulo.

Rizov, V. I., 2006a. Non-linear indentation behavior of foam core sandwich composite materials - A 2D approach. *Computational Materials Science*, v. 35, p. 107.

Rizov, V. I., 2006b. Elastic–plastic response of structural foams subjected to localized static loads. *Materials and Design*, v. 27, p. 947.

Russo, A.; Zuccarello, B., 2007. Experimental and numerical evaluation of the mechanical behaviour of GFRP sandwich panels. *Composite Structures*, v. 81, p. 575.

Sadighi, M.; Pouriayevali, H.; Saadati, M., 2007. A study of indentation energy in three points bending of sandwich beams with composite laminated faces and foam core. *World Academy of Science, Engineering and Technology*, v. 36, p. 214.

Shipsha, A.; Hallström, S.; Zenkert, D., 2003. Failure mechanisms and modeling of impact damage in sandwich beams - A 2D Approach: Part I - Experimental investigation. *Journal of Sandwich Structures and Materials*, v. 5, p. 7.

Soden, P. D., 1996. Indentation of composite sandwich beams. *Journal of Strain Analysis*, v. 31, n. 5, p. 353.

Sokolinsky, V. S.; Shen, H.; Vaikhanski, L.; Nuttet, S. R., 2004. Experimental and analytical study of nonlinear bending response of sandwich beams. *Composite Structures*, v. 60, p. 219.

Steeves, C. A.; Fleck, N. A., 2004a. Collapse mechanisms of sandwich beams with composite faces and a foam core, loaded in three-point bending. Part I: Analytical models and minimum weight design. *International Journal of Mechanical Sciences*, v. 46, p. 561.

Steeves, C. A.; Fleck, N. A., 2004b. Collapse mechanisms of sandwich beams with composite faces and a foam core, loaded in three-point bending. Part II: Experimental investigation and numerical modeling. *International Journal of Mechanical Sciences*, v. 46, p. 585.

Swanson, S. R.; Kim, J., 2002. Optimization of sandwich beams for concentrated loads. *Journal of Sandwich Structures and Materials*, v. 4, p. 273.

Tagarielli, V.L.; Fleck, N.A.; Deshpande, V.S., 2004. Collapse of clamped and simply supported composite sandwich beams in three-point bending. *Composites:* part B, v. 35, p. 523.

Tita, V.; Caliri Jr, M. F., 2013. Anisotropic mechanical behavior of polymeric foams. *Plastics Research Online - Society of Plastics Engineers (SPE)*, USA, 24 apr.

Tita, V.; Caliri Junior, M.F., 2012. Numerical simulation of anisotropic polymeric foams. *Latin American Journal of Solids and Structures*, v. 9, p. 259-279.

Tita, V.; Caliri Junior, M.F.; Angelico, R. A.; Canto, R. B., 2012. Experimental analyses of the poly (vinyl chloride) foams' mechanical anisotropic behavior. *Polymer Engineering and Science*, v. 52, p. 2654-2663.

Triantafillou, T. C.; Zhang, J.; Shercliff, T. L.; Gibson, L. J.; Ashby, M. F., 1989. Failure surfaces for cellular materials under multiaxial loads -II. Comparison of models with experiment. *International Journal of Mechanical Sciences*, v. 31, n. 9, p. 665.

Wang, D. -A.; Pan, J., 2006. A non-quadratic yield function for polymeric foams. *International Journal of Plasticity*, v. 22, p. 434.

Weaire, D.; Hutzler, S., 1999. *The physics of foams*. New York: Oxford University Press.

Yang, J.; Shen, H. -S.; Zhang, L., 2001. Nonlinear local response of foam-filled sandwich plates with laminated faces under combined transverse and in-plane loads. *Composite Structures*, v. 52, p. 137.

Zenkert, D.; Shipsha, A.; Persson, K., 2004. Static indentation and unloading response of sandwich beams. *Composites: Part B*, v. 35, p. 511.

Zhang, J.; Kikuchi, N.; Li, V.; Yee, A.; Nusholtz, G.,1998. Constitutive modeling of polymeric foam material subjected to dynamic crash loading. *International Journal of Impact Engineering*, v. 21, n. 5, p. 369.

8. RESPONSIBILITY NOTICE

The authors are the only responsible for the printed material included in this paper.